

## Structure stability towards cation substitutions in $A_2B_2O_5$ perovskites with crystallographic shear planes

P. Tzvetkov<sup>1,\*</sup>, D. Kovacheva<sup>1</sup>, D. Nihtianova<sup>1,2</sup>, T. Ruskov<sup>3</sup>

<sup>1</sup> Institute of General and Inorganic Chemistry, Bulgarian Academy of Sciences  
1113 Sofia "Acad. Georgi Bonchev" str. bld.11

<sup>2</sup> Institute of Mineralogy and Crystallography, Bulgarian Academy of Sciences  
1113 Sofia "Acad. Georgi Bonchev" str. bld.107

<sup>3</sup> Institute for Nuclear Research and Nuclear Energy, Bulgarian Academy of Sciences  
1784 Sofia "Tzarigradsko chaussee" 72 Blvd.

Received January 14, 2011; Revised March 4, 2011

New perovskite-related compounds with general formula  $Pb_{2-x}Ba_xFe_{2-y}Co_yO_5$  ( $0.67 \leq x \leq 1$ ,  $0 \leq y \leq 1$ ) were prepared by solution-combustion technique. The compounds were characterized by X-ray powder diffraction, SAED TEM, and  $^{57}\text{Fe}$  Mössbauer spectroscopy. The structure is closely related to other perovskite-derived structures such as  $\text{Ca}_2\text{FeAlO}_5$  and  $\text{Ca}_2\text{Mn}_2\text{O}_5$  and can be described as an anion deficient perovskite in which half of the  $B^{3+}$  cations are located in the octahedral coordination as in the prototype perovskite structure and the other half are five-coordinated in distorted tetragonal pyramids. The pyramidal coordination is formed by glide of one perovskite block in respect to the previous one at  $b/2$  along  $[010]$  direction as a result of ordered oxygen vacancies. The pyramids share common edges and form double chains and channels between them along the  $b$ -axis. Inside the channels there are  $\text{Pb}^{2+}$  cations that are located coordinated by six oxygen atoms and one  $6s^2$  electron lone pair of the lead atom. The second cation position is situated within the perovskite block and has mixed occupancy by the larger  $\text{Pb}^{2+}$  and  $\text{Ba}^{2+}$  ions. The study reveals that substitution of iron by cobalt is possible only at high substitution levels of lead by barium. The influence of the composition on the structural parameters and stability of the structure is discussed.

**Key words:** perovskites, crystallographic shear planes, cation substitutions.

### 1. INTRODUCTION

The perovskite structure is typical for compounds with general formula  $\text{ABX}_3$ , where  $A^+$  is cation with ionic radius close to that of the anion  $X^-$  (oxygen or halide anion) and  $B^+$  is a smaller cation usually of a transitional metal. The structure can be described as cubic close packing of  $A^+$  and  $X^-$  ions, where  $B^+$  is occupying  $1/4$  of the octahedral interstices. Since perovskite structure is very flexible towards modification of the composition and topological changes perovskite-type materials exhibit great variety of physical and chemical properties. Among the perovskites one can find typical dielectrics, high temperature superconductors, ion conductors, colossal magneto-resistant materials, optical materials, catalysts, etc. Many structures can be derived from that of perovskite by different ways: by mixed occu-

pancy and cation ordering in A and B position; vacancy ordering in the anion sublattice; intergrowth of perovskite and other structure type blocks (e.g.  $\text{NaCl}$ ,  $\text{CaF}_2$ ), and the formation of hexagonal perovskite polytypes, thus, leading to a huge number of compounds. Complex structural phenomena concerning the anion sublattice of the perovskites were observed and studied with regard to their influence on the physical properties of the materials. Among them are the oxygen vacancy distribution, ordering and evolution [1–4] and the formation of crystallographic shear planes [4–6]. The shear operation changes the connectivity scheme of the metal-oxygen polyhedra, replacing corner-sharing  $\text{BO}_6$  octahedra by edge-sharing  $\text{BO}_5$  distorted tetragonal pyramids. The introduction of periodically ordered translational interfaces into the perovskite structure was performed on the basis of detailed transmission electron microscopy investigations of a new class of Pb and Fe-containing compounds [6–8]. These compounds are closely related to the brownmillerite-type structure and are isostructural with

\* To whom all correspondence should be sent:  
E-mail: p-tzvetkov@gmx.net

$\text{Pb}_{1.33}\text{Sr}_{0.67}\text{Fe}_2\text{O}_5$  ( $Pnma$ ,  $a = 5.687$ ,  $b = 3.920$ ,  $c = 21.075$  Å) [9]. The structure is complex due to the fragmentation of the perovskite matrix. The corner sharing  $\text{FeO}_6$  octahedra alter with double chains of edge sharing mirror-related  $\text{FeO}_5$  distorted tetragonal pyramids. The  $\text{FeO}_5$  chains running along the  $b$ -axis and the octahedra of the perovskite blocks delimit six-sided tunnels, where Pb atoms are located. Two configurations of  $\text{FeO}_5$  chains occur, arbitrary denoted as L- and R-chains. At room temperature they are fully ordered and alternate along the  $c$ -axis. A phase transition between an ordered and disordered arrangement of the chains was detected in  $\text{PbBaFe}_2\text{O}_5$  around 270 °C [10]. The Sr(Ba) and Pb atoms occupy mixed positions located in the cuboctahedral cavities inside the perovskite blocks. The accommodation of lone  $6s^2$  electron pair ( $\text{Pb}^{2+}$ ,  $\text{Bi}^{3+}$ ) in the A position of the perovskite structure is a condition for ferroelectric properties. In addition, the coordination of  $\text{Fe}^{3+}$  in the structure with B–O–B angles of 180° and 90° can lead to unusual magnetic behavior [6]. The perovskite structure is flexible and accommodates variety of substitutions.

The purpose of the present work is to study the tolerance toward cation substitutions in A and B positions of the perovskite structure modified by translational interfaces (crystallographic shear planes). We report the synthesis and structural characterization of a new series of polycrystalline compounds with general formula  $\text{Pb}_{2-x}\text{Ba}_x\text{Fe}_{2-y}\text{Co}_y\text{O}_5$  ( $0.67 \leq x \leq 1$ ,  $0 \leq y \leq 1$ ).

## 2. EXPERIMENTAL

Polycrystalline samples with chemical composition  $\text{Pb}_{2-x}\text{Ba}_x\text{Fe}_{2-y}\text{Co}_y\text{O}_5$  ( $0.67 \leq x \leq 1$ ,  $0 \leq y \leq 1$ ) were prepared by the solution-combustion technique [11, 12]. The starting compounds used were  $\text{Fe}(\text{NO}_3)_3 \cdot 9\text{H}_2\text{O}$ ,  $\text{Pb}(\text{NO}_3)_2$ ,  $\text{Ba}(\text{NO}_3)_2$ ,  $\text{Co}(\text{NO}_3)_2 \cdot 6\text{H}_2\text{O}$  and sucrose ( $\text{C}_{12}\text{H}_{22}\text{O}_{11}$ ), all of analytical grade purity. A stoichiometric mixture of the reagents was dissolved in a minimum quantity of distilled water. The dish containing the reaction mixture was placed on an electric heater and evaporated until drying. After drying, the samples were left on the heater to raise the temperature and initialize the combustion reaction. The samples burned quickly, forming light fine powders. The obtained powders were further homogenized in agate mortar and heated at 400°C for 2 hours in order to burn the organic residue, homogenized again and pressed into pellets (14 mm diameter) at 714 atm [ $\text{kg}/\text{cm}^2$ ] pressure. The pellets were placed into corundum crucibles and heated for 24 hours at 850 °C in air with one intermediate grinding after the first 12 hours. The samples were grinded and heated again at 930 °C for 1 hour in

order to promote the reaction of  $\text{BaPbO}_3$  detected as a minor impurity phase in the samples.

Mössbauer spectra were taken in the transmission mode at room temperature using a constant acceleration spectrometer. A source of  $^{57}\text{Co}(\text{Rh})$  was used.  $\text{PbBaFe}_{2-x}\text{Co}_x\text{O}_5$  ( $x = 0, 0.5, 1$ ) powder material was mixed with polyvinyl alcohol powder (glue substance) and then pressed into a disk. The thickness of the disk was chosen to achieve Mössbauer absorber thickness of 50  $\text{mg cm}^{-2}$ . The spectra were fitted using an integral Lorentzian line shape approximation [13, 14]. The isomer shifts are referred to the centroid of  $\alpha$ -iron foil reference spectrum at room temperature. The geometric effect was taken into account.

The TEM investigations for  $\text{PbBaFe}_{2-x}\text{Co}_x\text{O}_5$  ( $x = 0.5, 1$ ) were performed by TEM JEOL 2100 with 200 kV accelerating voltage. The specimens were grinded and dispersed in ethanol by ultrasonic treatment for 6 min. The suspensions were dripped on standard holey carbon/Cu grids.

Powder X-ray diffraction patterns were collected at room temperature on Bruker D8 Advance diffractometer using  $\text{CuK}\alpha$  radiation and LynxEye PSD detector within the range 5–140°  $2\theta$ , step 0.02°  $2\theta$  and 6 sec/strip (total of 1050 sec/step). To improve the statistics, rotating speed of 60 rpm was used. The crystal structure parameters were refined using TOPAS 3 program [15].

## 3. RESULTS AND DISCUSSION

According to the results of the powder XRD analyses it was found that the substitution of cobalt for iron in the structure of  $\text{Pb}_{2-x}\text{Ba}_x\text{Fe}_2\text{O}_5$  depends strongly on the degree of substitution of lead by barium. For  $x < 0.9$  only small amount of cobalt can be accommodated in the structure. With the increase of the substitution level to  $x = 1$  a solid solution series with composition  $\text{PbBaFe}_{2-x}\text{Co}_x\text{O}_5$  ( $x = 0, 0.25, 0.5, 0.75, 1$ ) was successfully synthesized. Unit cell parameters of the corresponding phases are presented in Table 1. The substitution leads to slight increase of  $b$  parameter and simultaneous decrease of both  $a$  and  $c$  parameters. As a result, the volume of the unit cell decreases with the increase of the substitution level. This fact is consistent with the difference of the ionic radii of  $\text{Fe}^{3+}$  (0.645 Å) and  $\text{Co}^{3+}$  (0.61 Å) [16].

The Rietveld refinement of the compounds within the series  $\text{PbBaFe}_{2-x}\text{Co}_x\text{O}_5$  ( $x = 0, 0.25, 0.5, 0.75, 1$ ) revealed that they all are isostructural with the end member  $\text{PbBaFe}_2\text{O}_5$ . Detailed structural parameters for the composition  $\text{PbBaFeCoO}_5$  are presented in Table 2. Due to the small difference of the atomic scattering factors of  $\text{Fe}^{3+}$  and  $\text{Co}^{3+}$ , the distribution of

**Table 1.** Unit-cell parameters for the  $\text{PbBaFe}_{1-x}\text{Co}_x\text{O}_5$  solid solutions calculated from XRD data

| $x$  | $a$ (Å)    | $b$ (Å)    | $c$ (Å)    | $V$ (Å <sup>3</sup> ) |
|------|------------|------------|------------|-----------------------|
| 0.00 | 5.76504(6) | 3.99197(4) | 21.1376(2) | 486.440(9)            |
| 0.25 | 5.76277(6) | 3.99414(5) | 21.0965(2) | 485.62(1)             |
| 0.50 | 5.76075(5) | 3.99950(4) | 21.0468(2) | 484.96(1)             |
| 0.75 | 5.75921(4) | 4.00445(3) | 20.9975(2) | 484.297(7)            |
| 1.00 | 5.75834(4) | 4.00866(3) | 20.9558(2) | 483.745(9)            |

**Table 2.** Refined structural parameters for  $\text{PbBaFeCoO}_5$ , space group  $Pnma(62)$ ,  $a = 5.75834(4)$ ,  $b = 4.00866(3)$ ,  $c = 20.9558(2)$ ,  $Z = 4$ 

| Atom  | Wyck. | x/a       | y/b | z/c        | SOF  | $B_{\text{iso}}$ (Å <sup>2</sup> ) |
|-------|-------|-----------|-----|------------|------|------------------------------------|
| Pb(1) | 4c    | 0.0051(8) | 1/4 | 0.56867(7) | 1.00 | 0.69(3)                            |
| Ba(2) | 4c    | 0.4888(9) | 1/4 | 0.68424(9) | 1.00 | 0.44(5)                            |
| Fe(1) | 4c    | 0.521(2)  | 1/4 | 0.4463(2)  | 1.00 | 0.38(6)                            |
| Co(2) | 4c    | 1.000(2)  | 1/4 | 0.3155(3)  | 1.00 | 0.38(6)                            |
| O(1)  | 4c    | 0.962(4)  | 3/4 | 0.3188(7)  | 1.00 | 1.3(2)                             |
| O(2)  | 4c    | 0.728(4)  | 1/4 | 0.235(1)   | 1.00 | 1.3(2)                             |
| O(3)  | 4c    | 0.201(4)  | 1/4 | 0.394(2)   | 1.00 | 1.3(2)                             |
| O(4)  | 4c    | 0.747(4)  | 1/4 | 0.387(2)   | 1.00 | 1.3(2)                             |
| O(5)  | 4c    | 0.542(4)  | 3/4 | 0.4608(6)  | 1.00 | 1.3(2)                             |

$$R_B = 1.46, R_{\text{wp}} = 3.52, R_{\text{exp}} = 1.09, \text{GOF} = 3.23$$

cobalt over the two possible cation sites could not be determined from the XRD experiments. Therefore, a Mössbauer spectroscopy was performed.

The Mössbauer spectra of the two types of samples  $\text{PbBaFe}_2\text{O}_5$  (Type I) and  $\text{PbBaFe}_{1.5}\text{Co}_{0.5}\text{O}_5$  (Type II) are shown in Fig. 1. The fitted parameters corresponding to isomer shift (IS), full width at half maximum (FWHM) of the absorption lines, quadrupole shift (QS), magnetic field at the site of the Fe nucleus (H), and relative spectral area are summarized in Table 3.

Each spectrum was fitted by superposition of two well-resolved magnetic Zeeman sextets, (1) and

(2), corresponding to the two positions of the iron in the crystal lattice of the investigated material. For the first sample (that without Co) we obtained the isomer shift of the sextet (1) as 0.329 mm/s, while for the sextet (2) it is 0.418 mm/s. For the second sample (with Co) the isomer shifts are 0.33 mm/s and 0.42 mm/s, respectively. Therefore, within the experimental error, there is no difference as to the isomer shift for the two samples. In both positions the valence state of the iron is  $\text{Fe}^{3+}$ . However, in general, taking into account the systematic decrease of the isomer shift on decreasing of the coordination of iron, we should assign, for both types of samples,

**Table 3.**  $^{57}\text{Fe}$  Mossbauer spectral parameters of hyperfine interaction for  $\text{PbBaFe}_2\text{O}_5$  and  $\text{PbBaFe}_{1.5}\text{Co}_{0.5}\text{O}_5$ 

| Sample  | Site | IS [mm/s] | FWHM [mm/s] | QS [mm/s] | H [kOe]  | Relative area [%] |
|---------|------|-----------|-------------|-----------|----------|-------------------|
| Type I  | 1    | 0.329(3)  | 0.17(1)     | 0.107(3)  | 434.6(3) | 50.7 ± 1.4        |
|         | 2    | 0.418(3)  | 0.18(1)     | -0.106(4) | 502.5(2) | 49.3 ± 1.4        |
| Type II | 1    | 0.33(1)   | 0.26(2)     | 0.128(6)  | 431.6(4) | 46.6 ± 1.8        |
|         | 2    | 0.42(1)   | 0.25(2)     | -0.106(5) | 496.2(3) | 53.4 ± 1.8        |

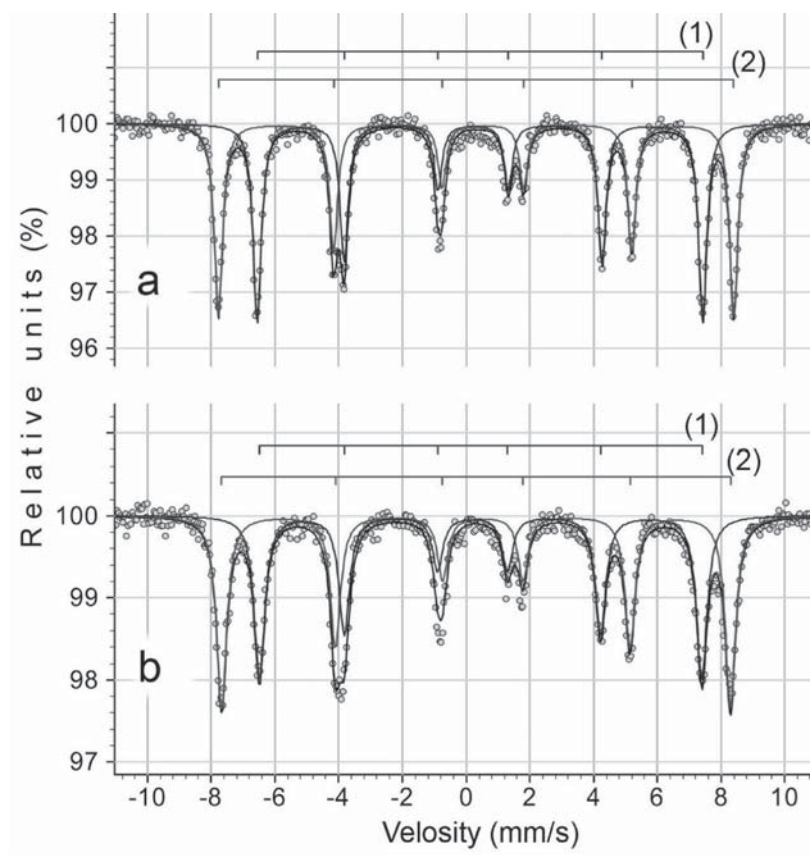


**Fig. 1.** Mössbauer spectra of  $\text{PbBaFe}_2\text{O}_5$  (a) and  $\text{PbBaFe}_{1.5}\text{Co}_{0.5}\text{O}_5$  (b)

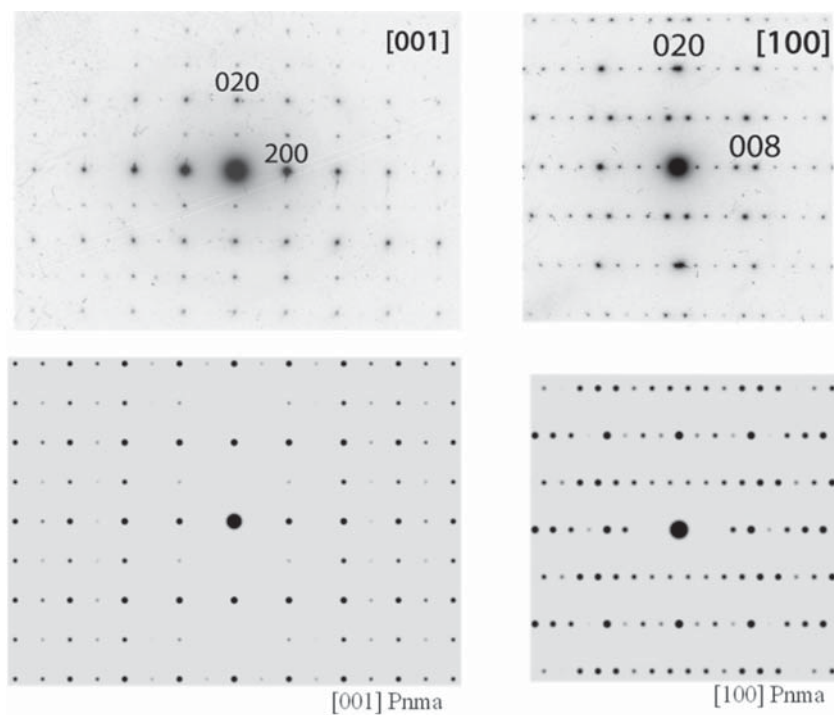


**Fig. 2.** Experimental and calculated selected area electron diffraction patterns of  $\text{PbBaFeCoO}_5$  in  $[001]$  and  $[100]$  directions

sextet (1) to the pyramidal site ( $\text{Fe-O}_5$ ) and sextet (2) to the octahedral site ( $\text{Fe-O}_6$ ) [14]. The sample with Co shows a significant increase of the resonance line width for both sites: the pyramidal and octahedral ones. There is also a small decrease of the magnetic field at the site of the Fe nucleus when going from Type I (without Co) to Type II (with Co) samples. It should be mentioned some difference of the relative spectral area as well. The sample without Co shows

nearly equal spectral area for both sites, while the sample with Co shows that the pyramidal site is several percent less populated by iron (Fig. 1 and Table 3).

Summarizing all the data we can conclude that cobalt replaces iron in both sites, but with more preference to the pyramidal one. The broadening of the resonance lines for Type II sample is connected with the random distribution of cobalt and different

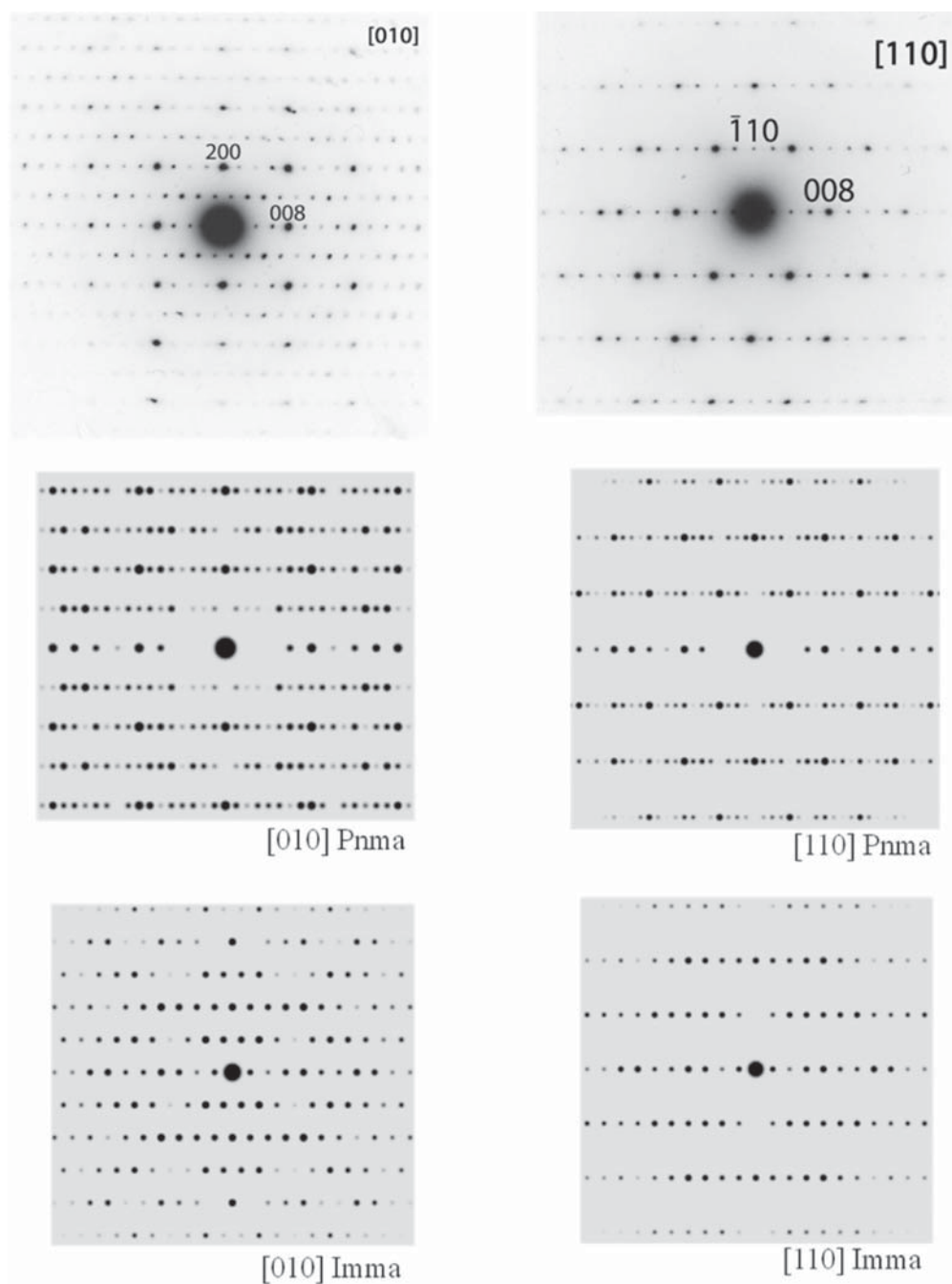


**Fig. 3.** Experimental and calculated selected area electron diffraction patterns of  $\text{PbBaFeCoO}_5$ . In directions [010] and [110] both low ( $Pnma$ ) and high ( $Imma$ ) temperature phases are observed

exchange interactions Fe–Fe and Fe–Co. The small increase of the cobalt population in the pyramidal site could be explained by the different ion radii of Fe and Co. The cobalt ion has a smaller radius than the iron ion and it is easier for Co ion to be placed into the pyramidal site than iron ion since the pyramidal site volume is smaller than that of the octahedral site. The asymmetric population of cobalt in the octahedral and pyramidal sites is an additional way to assign magnetic sextet (1) to the pyramidal site (Fe-O<sub>5</sub>) and sextet (2) to the octahedral site (Fe-O<sub>6</sub>).

Experimental and calculated SAED patterns of sample PbBaFeCoO<sub>5</sub> are shown in Figs. 2 and 3. The complete indexing of the patterns was performed using an orthorhombic unit cell as determined from the XRD data. The reflection conditions:  $0kl:k+l = 2n$ ,  $hk0:h = 2n$ ,  $h00:h = 2n$ ,  $0k0:k = 2n$ ,  $00l:l = 2n$  are unambiguously derived from the [100] and [001] electron diffraction patterns, in agreement with the proposed *Pnma* space group.

The parent structure PbBaFe<sub>2</sub>O<sub>5</sub> undergoes a phase transition from *Pnma* to *Imma* space group at 270 °C [10]. The same transition was observed for the substituted sample PbBaFeCoO<sub>5</sub> during the TEM studies. The SAED patterns for [010] and [110] directions can be indexed by using two sets of diffraction patterns – one for the low-temperature phase and a second one for the high-temperature phase. We suppose that this transition is caused by the electron beam irradiation. Experimental [100], [010], [001], [110] SAED patterns are compared with calculated ones and a good accordance is observed.

**Acknowledgements:** The authors thank the National Science Fund of Bulgaria (Grant DO-02-224/17.12.2008)

for the financial support. D. Nihtianova and T. Ruskov thanks Grant No DTK-02/77/22.12.2009).

## REFERENCES

1. M. Anderson, J. Vaughey, K. Poeppelmeier, *Chem. Mater.*, **5**, 151 (1993).
2. J. Vaughey, K. Poeppelmeier, *NIST Special Publication*, **804**, 419 (1991).
3. J. Hadermann, G. Van Tendeloo, A. Abakumov, *Acta Cryst. A*, **61**, 77 (2005).
4. E. Antipov, A. Abakumov, S. Istomin, *Inorg. Chem.*, **47**, 8543 (2008).
5. C. Bougerol, M. Gorius, I. Grey, *J. Solid State Chem.*, **169**, 131 (2002).
6. A. Abakumov, J. Hadermann, S. Bals, I. Nikolaev, E. Antipov, G. Van Tendeloo, *Angew. Chem. Int. Ed.*, **45**, 6697 (2006).
7. A. Abakumov, J. Hadermann, G. Van Tendeloo, E. Antipov, *J. Am. Ceram. Soc.*, **91**, 1807 (2008).
8. G. Van Tendeloo, J. Hadermann, A. Abakumov, E. Antipov, *J. Mater. Chem.*, **19**, 2660 (2009).
9. V. Raynova-Schwarten, W. Massa, D. Babel, *Z. Anorg. Allg. Chem.*, **623**, 1048 (1997).
10. I. Nikolaev, H. D'Hondt, A. Abakumov, J. Hadermann, A. Balagurov, I. Bobrikov, D. Sheptyakov, V. Pomjakushin, K. Pokholok, D. Filimonov, G. Van Tendeloo, E. Antipov, *Phys. Rev. B*, **78**, 024426 (2008).
11. M. Sekar, K. Pathil, *J. Mater. Chem.*, **2**, 739 (1992).
12. K. Patil, S. Aruna, T. Mimani, *Curr. Opin. Solid State Mater. Sci.*, **6**, 507 (2007).
13. G. Shenoy, J. Friedt, H. Maleta, S. Ruby, *Mössbauer Effect Methodology*, **9**, 277 (1974).
14. T. Cranshaw, *J. Phys. E*, **7**, 122 (1974).
15. TOPAS 3: General profile and structure analysis software for powder diffraction data, Bruker AXS, Karlsruhe, Germany. Menil, F., 1985, *J. Phys. Chem. Solids*, **46**, 763 (2005).
16. R. Shannon, *Acta Cryst. A*, **32**, 751 (1976).

## СТРУКТУРНА СТАБИЛНОСТ И КАТИОННО ЗАМЕСТВАНЕ В $A_2B_2O_5$ ПЕРОВСКИТИ С КРИСТАЛОГРАФСКИ РАВНИНИ НА СРЯЗВАНЕ

П. Цветков<sup>1,\*</sup>, Д. Ковачева<sup>1</sup>, Д. Нихтянова<sup>1,2</sup>, Т. Русков<sup>3</sup>

<sup>1</sup> *Институт по обща и неорганична химия, Българска академия на науките  
1113 София ул. „Акад. Георги Бончев“ бл.11*

<sup>2</sup> *Институт по минералогия и кристалография, Българска академия на науките  
1113 София ул. „Акад. Георги Бончев“ бл.107*

<sup>3</sup> *Институт за ядрени изследвания и ядрена енергия, Българска академия на науките 1784 София бул.  
„Цариградско шосе“ 72*

Постъпила на 14 януари, 2011 г.; приета на 4 март, 2011 г.

(Резюме)

Чрез метода на комбустия от разтвор бяха синтезирани нови перовскитоподобни съединения с обща формула  $Pb_{2-x}Ba_xFe_{2-y}Co_yO_5$  ( $0.67 < x < 1$ ,  $0 < y < 1$ ). Веществата са характеризирани с X-ray прахова дифракция, SAED ТЕМ и  $^{57}Fe$  Mössbauer спектроскопия. Структурата е близка на други производни структури като  $Ca_2FeAlO_5$  и  $Ca_2Mn_2O_5$  и може да бъде описана като анионно дефицитен перовскит, в който половината от  $B^{3+}$  катиони заемат октаедрична координация, а останалата половина са в петорна координация в изкривени тетрагонални пирамиди. Петорната координация на пирамидите се получава от прихлъзване на един перовскитов блок спрямо съседния на  $b/2$  по направление  $[010]$ , като резултат от подредени кислородни ваканции. Пирамидите споделят общи ръбове и образуват двойни вериги и канали по дължина на  $b$ -оста. Вътре в каналите  $Pb^{2+}$  катиони са координирани от шест кислородни атома и една  $6s^2$  електронна двойка от оловния атом. Втората голяма катионна позиция се намира в перовскитовия блок и има смесено заселване от  $Pb^{2+}$  и  $Ba^{2+}$  иони. Изследването показва, че заместването на желязо с кобалт е възможно само при високи нива на заместване на олово от барий. Обсъдени са влиянието на състава върху структурните параметри и стабилността на структурата.